Mitofusin 2 (Mfn2) links mitochondrial and endoplasmic reticulum function with insulin signaling and is essential for normal glucose homeostasis

David Sebastián[a,b,c,1], María Isabel Hernández-Alvarez[a,b,c,1], Jessica Segalés[a,b,c,1], Eleonora Sorianello[a,b,c], Juan Pablo Muñoz[a,b,c], David Sala[a,b,c], Aurélie Waget[d], Marc Liesa[a,b,c], José C. Paz[a,b,c], Peddinti Gopalacharyulu[e], Matej Orešič[e], Sara Pich[a,b], Rémy Burcelin[d], Manuel Palacín[a,b], and Antonio Zorzano[a,b,c,2]

[a]Institute for Research in Biomedicine (IRB Barcelona), 08028 Barcelona, Spain; [b]Departament de Bioquímica i Biologia Molecular, Facultat de Biologia, Universitat de Barcelona, 08028 Barcelona, Spain; [c]Instituto de Salud Carlos III, Centro de Investigación Biomédica en Red de Diabetes y Enfermedades Metabólicas Asociadas (CIBERDEM), 08017 Barcelona, Spain; [d]Institut National de la Santé et de la Recherche Médicale Unité 1048, Institut de Recherche sur les Maladies Métaboliques et Cardiovasculaires de l'Hôpital Rangueil, 31432 Toulouse, France; and [e]Quantitative Biology and Bioinformatics, VTT Technical Research Centre of Finland, 02044 Espoo, Finland

Edited* by Bruce M. Spiegelman, Dana-Farber Cancer Institute and Harvard Medical School, Boston, MA, and approved February 7, 2012 (received for review June 21, 2011)

Mitochondria are dynamic organelles that play a key role in energy conversion. Optimal mitochondrial function is ensured by a quality-control system tightly coupled to fusion and fission. In this connection, mitofusin 2 (Mfn2) participates in mitochondrial fusion and undergoes repression in muscle from obese or type 2 diabetic patients. Here, we provide in vivo evidence that Mfn2 plays an essential role in metabolic homeostasis. Liver-specific ablation of Mfn2 in mice led to numerous metabolic abnormalities, characterized by glucose intolerance and enhanced hepatic gluconeogenesis. Mfn2 deficiency impaired insulin signaling in liver and muscle. Furthermore, Mfn2 deficiency was associated with endoplasmic reticulum stress, enhanced hydrogen peroxide concentration, altered reactive oxygen species handling, and active JNK. Chemical chaperones or the antioxidant *N*-acetylcysteine ameliorated glucose tolerance and insulin signaling in liver-specific Mfn2 KO mice. This study provides an important description of a unique unexpected role of Mfn2 coordinating mitochondria and endoplasmic reticulum function, leading to modulation of insulin signaling and glucose homeostasis in vivo.

mitochondrial dynamics | insulin resistance | metabolism | oxidative stress

Mitochondrial morphology, response to apoptotic stimuli, mitochondrial metabolism, and quality control are in part controlled through the balance between mitochondrial fusion and fission (1, 2). Mitochondrial fusion in mammalian cells is controlled by mitofusin 1 and 2 (Mfn1 and Mfn2) proteins and by optic atrophy 1 (OPA1). Mfn1 and Mfn2 explain outer mitochondrial membrane fusion. Mfn2 has pleiotropic cellular roles and regulates cell proliferation, oxidative metabolism, autophagy, and mitochondrial antiviral signaling protein (3–7). In addition, Mfn2 is also localized in the endoplasmic reticulum (ER)–mitochondrial contact sites, and it regulates the tethering of the ER to mitochondria as well as calcium homeostasis in mouse embryonic fibroblasts (8). Double ablation of Mfn2 and Mfn1 causes mitochondrial DNA depletion, indicating that these proteins are required for mitochondrial DNA stability (9). Mfn2 is relevant in human disease, and mutations in Mfn2 have been reported in patients affected by Charcot–Marie–Tooth neuropathy type 2A (10–12). In addition, we have reported that Mfn2 expression is reduced in skeletal muscle of obese subjects and in type 2 diabetic patients (13, 14).

Insulin resistance in skeletal muscle and liver plays a primary role in the pathogenesis of type 2 diabetes (15). There is substantial evidence in humans indicating that insulin-resistant conditions are characterized by alterations in mitochondrial activity in skeletal muscle caused by either reduced mitochondrial mass or functional impairment of mitochondria (16–19). However, several studies have challenged the concept that insulin resistance is caused by a deficient mitochondrial function (20–22). Alternatively, insulin resistance may be a consequence of specific alterations in mitochondrial metabolism. In this regard, a high-fat diet (HFD) causes increased hydrogen peroxide production and oxidative stress in skeletal muscle, which might explain, at least in part, the development of insulin resistance (23, 24). On the basis of these studies, we sought to determine the effects of Mfn2 in mitochondrial function and glucose homeostasis in vivo. We demonstrate that Mfn2 deficiency produces mitochondrial dysfunction, increases H_2O_2 concentration, and activates JNK, leading to insulin resistance in skeletal muscle and liver. Importantly, Mfn2 deficiency also leads to ER stress, contributing as well to the loss of insulin sensitivity. In this paper, we describe a unique mechanism by which mitochondrial and ER function, both under the control of Mfn2, converge in the regulation of insulin signaling and glucose homeostasis in vivo.

Results

Liver-Specific Mfn2 KO Mice Show Glucose Intolerance, Enhanced Hepatic Glucose Production, and Impaired Response to Insulin. Liver-specific Mfn2 KO mice were generated, and expression of Mfn2 was analyzed in tissues from control (Alb-Cre$^{-/-}$ Mfn2$^{loxP/loxP}$) and KO (Alb-Cre$^{+/-}$ Mfn2$^{loxP/loxP}$; hereafter referred to as L-KO) mice. Mfn2 expression was absent in liver, whereas normal Mfn2 expression was detected in other tissues (Fig. 1*A*). Isolation of mouse hepatocytes was performed to analyze the architecture of the mitochondrial network. Mitochondria formed tubules in control hepatocytes, whereas mitochondrial clusters were detected in L-KO mice (Fig. 1*B*). L-KO mice at 8 wk of age showed similar values of body weight or epididymal adipose depots compared with control mice (Fig. S1 *A* and *B*). Plasma glucose was increased in Mfn2 KO mice under a normal chow diet (Fig. 1*C*), which occurred in the presence of normal plasma insulin or glucagon levels (Fig. 1 *D* and *E*). L-KO mice at 8 wk of age showed impaired glucose tolerance (Fig. 1*F*) without changes in plasma insulin levels (Fig. S1*C*). Glucose intolerance was also detected in L-KO mice subjected to a HFD for 20 wk (Fig. 1*G*), despite no changes in body weight (Fig. S1 *D* and *E*). In mice subjected to

Author contributions: D. Sebastián, M.I.H.-A., J.S., E.S., J.P.M., D. Sala, A.W., J.C.P., S.P., R.B., and A.Z. designed research; D. Sebastián, M.I.H.-A., J.S., E.S., J.P.M., D. Sala, J.C.P., P.G., and S.P. performed research; M.L. contributed new reagents/analytic tools; D. Sebastián, M.I.H.-A., J.S., E.S., J.P.M., D. Sala, J.C.P., M.O., S.P., R.B., M.P., and A.Z. analyzed data; and A.Z. wrote the paper.

The authors declare no conflict of interest.

*This Direct Submission article had a prearranged editor.

[1]D. Sebastián, M.I.H.-A., and J.S. contributed equally to this work.

[2]To whom correspondence should be addressed. E-mail: antonio.zorzano@irbbarcelona.org.

This article contains supporting information online at www.pnas.org/lookup/suppl/doi:10.1073/pnas.1108220109/-/DCSupplemental.

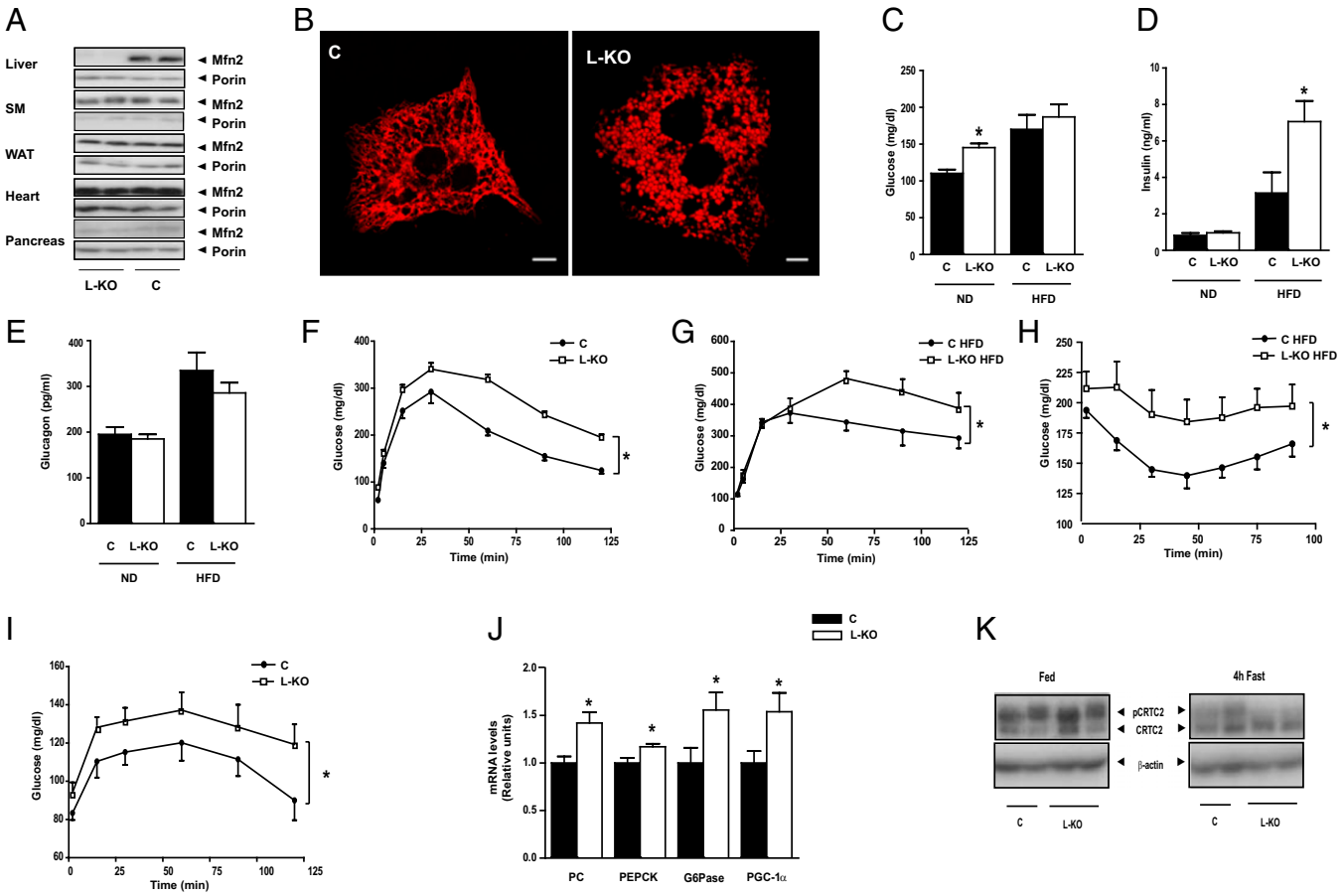

Fig. 1. Liver-specific Mfn2 ablation causes glucose intolerance and a reduced response to insulin. (*A*) Mfn2 protein levels from various tissues in control and L-KO mice. (*B*) Representative images of mitochondria in isolated hepatocytes. Mitochondria were visualized by transfecting hepatocytes with DsRed2-mito vector. (*C–E*) Plasma glucose insulin and glucagon levels in mice fed a normal diet (ND) or a HFD (n = 8–12). (*F*) Glucose tolerance test (GTT) on mice fed a normal diet (n = 15–20). (*G*) GTT on mice fed a HFD (n = 8–12). (*H*) Insulin tolerance tests on mice fed a HFD (n = 8–12). (*I*) Pyruvate challenge (n = 15–20). (*J*) Hepatic expression of gluconeogenic genes (n = 8–12). (*K*) CRTC2 phosphorylation in livers from fed or 4-h fasting mice. Data represent mean ± SEM. *P < 0.05. C, control; G6Pase, glucose 6-phosphatase; PC, pyruvate carboxylase.

a HFD, plasma glucose was similar in control and L-KO mice (Fig. 1*C*). In contrast, plasma insulin levels were markedly greater in L-KO mice (Fig. 1*D*). The L-KO mouse subjected to a HFD showed impaired glucose tolerance and high basal plasma insulin levels, suggesting susceptibility to insulin resistance. In keeping with this finding, insulin administration caused a lower hypoglycemic response in L-KO mice than in controls when subjected to a HFD (Fig. 1*H*).

The impaired glucose tolerance of L-KO mice was characterized by enhanced hepatic glucose production by gluconeogenesis (assessed by the pyruvate challenge test) (Fig. 1*I*) and by increased expression of genes encoding for gluconeogenic enzymes [pyruvate carboxylase, phosphoenolpyruvate carboxykinase (PEPCK), or glucose 6-phosphatase] and regulators of gluconeogenesis such as peroxisome proliferator-activated receptor γ coactivator 1α (PGC-1α) (Fig. 1*J*). These results suggest that Mfn2 loss of function increases the expression of cAMP-response element-binding (CREB) target genes (25). Next we studied the possibility that the nuclear factor CREB-regulated transcription coactivator 2 [CRTC2 (TORC2)] was activated by dephosphorylation in livers from L-KO mice. In the fed state, CRTC2 was mainly phosphorylated, and no differences were detected between control and Mfn2 KO mice (Fig. 1*K*). However, Mfn2 KO mice showed a greater response to 4 h of fasting so that most CRTC2 was dephosphorylated (Fig. 1*K*). No changes in the expression of forkhead box protein O1 (FoxO1) or hepatocyte nuclear factor 4 (HNF4) were detected (Fig. S2), but a reduced phosphorylation of FoxO1 was detected in the L-KO group after insulin treatment (Fig. S2*C*). These results suggest that Mfn2 deficiency causes a greater activation of CRTC2 and FoxO1 as well as the induction of target genes and gluconeogenesis.

Mef2C-Cre$^{+/-}$ Mfn2$^{loxP/loxP}$ Mice Show Higher Susceptibility to Developing Glucose Intolerance and Insulin Resistance in Response to Aging or HFD. Mfn2$^{loxP/loxP}$ mice were crossed with a mouse strain expressing Cre recombinase under the control of the MEF2C promoter (mef2C-73K-Cre) (26). The expression of Mfn2 was analyzed in control (mef2C-Cre$^{-/-}$ Mfn2$^{loxP/loxP}$) and KO (mef2C-Cre$^{+/-}$ Mfn2$^{loxP/loxP}$) mice. Mfn2 protein expression in the KO group was markedly reduced (80% decrease) in skeletal muscle, heart, and brain, and a near 50% reduction was detected in adipose tissues, kidney, or liver (Fig. 2*A*). Immunofluorescence analysis indicated that Mfn2 was markedly depleted in muscle fibers from mef2C-Cre$^{+/-}$ Mfn2$^{loxP/loxP}$ mice (Fig. 2*B*). Furthermore, skeletal muscle from mef2C-Cre$^{+/-}$ Mfn2$^{loxP/loxP}$ mice showed mitochondrial fragmentation compared with the control group, as assessed by confocal microscopy of muscles after in vivo gene transfer of DsRed2-Mito vector (Fig. 2*C*). At 24 wk old, Mfn2 KO mice showed unaltered values of body weight, epididymal adipose tissue, and plasma levels of glucose and insulin (Fig. S3 *A–D*) as well as normal glucose tolerance (Fig. S3*B*). However, 54-wk-old Mfn2 KO mice showed fasting hyperinsulinemia and high plasma insulin levels after a glucose challenge, in the presence of a normal glucose tolerance (Fig. 2 *D* and *E*) and normal body weight, indicating the existence

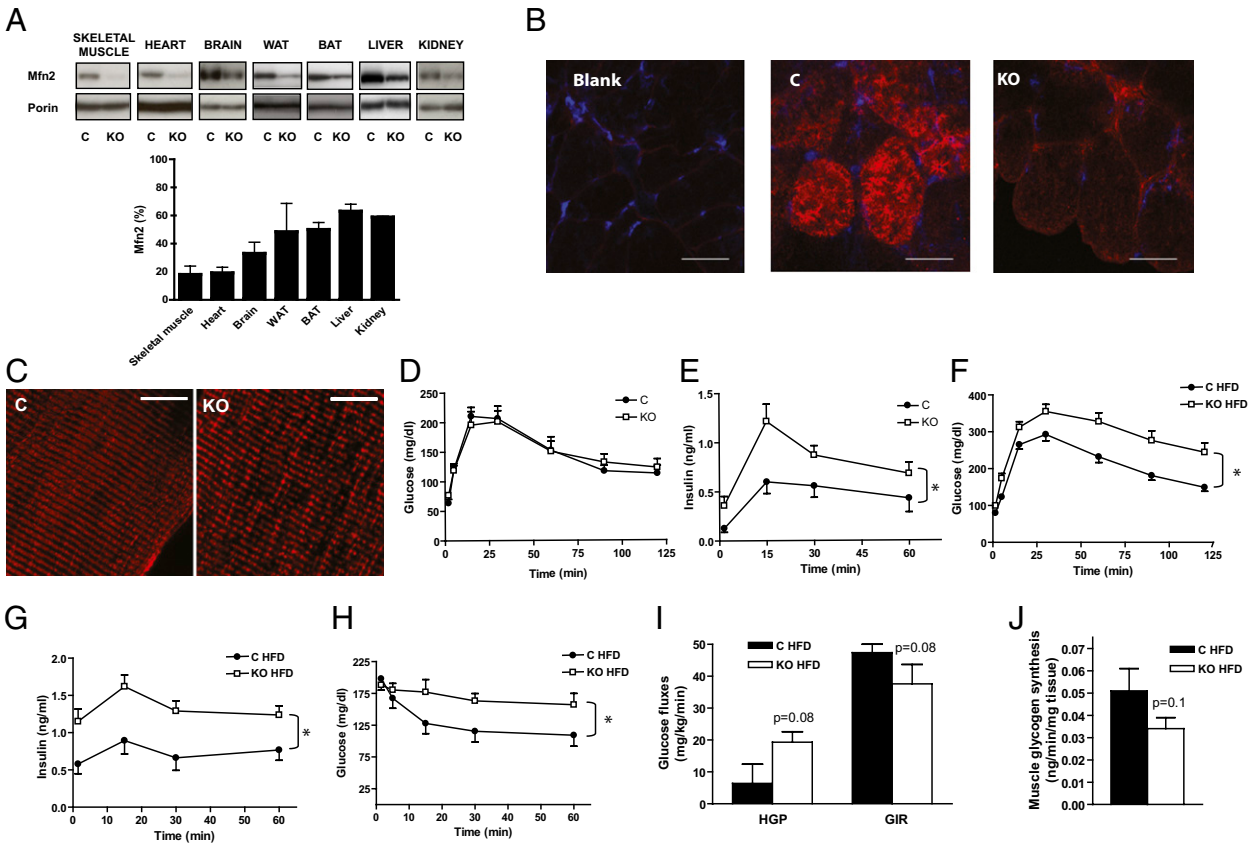

Fig. 2. Mfn2 KO mice show impaired glucose tolerance, high plasma insulin levels, and insulin resistance in response to aging or HFD. (*A*) Mfn2 protein levels in mitochondrial extracts from several tissues in control (C) and Mfn2 KO mice and densitometric quantification (n = 3–8). (*B*) Confocal images of intracellular localization of Mfn2 by immunofluorescence in transversal sections of gastrocnemius muscles of control and KO mice. (Scale bars: 50 μm.) (*C*) Mitochondrial network was visualized by confocal microscopy using longitudinal sections of tibialis anterior muscles expressing a DsRed2-Mito vector that specifically labels mitochondria. (Scale bars: 50 μm.) (*D*) GTT on 54-wk-old mice (n = 8). (*E*) Insulin levels during the GTT in 54-wk-old mice (n = 8). (*F*) GTT on mice subjected to a HFD for 14 wk (n = 8–12). (*G*) Insulin levels during the GTT in HFD-fed mice (n = 8–12). (*H*) Insulin tolerance test in mice subjected to a HFD for 14 wk (n = 8–12). (*I*) Glucose fluxes during the euglycemic-hyperinsulinemic clamp in HFD-fed mice (26 wk) (n = 5). (*J*) Muscle glycogen synthesis assessed during euglycemic-hyperinsulinemic clamp in mice fed a HFD (n = 5). Data represent mean ± SEM. *$P < 0.05$ vs. control mice.

of insulin resistance. After 14 wk on a HFD, Mfn2 KO mice showed impaired glucose tolerance compared with controls and higher plasma insulin levels, thereby suggesting a greater extent of insulin resistance (Fig. 2 *F* and *G*). In keeping with this finding, insulin caused a lower hypoglycemic response in Mfn2 KO mice than in controls when subjected to a HFD (Fig. 2*H*). The impact of Mfn2 ablation on whole-body glucose utilization was determined in conscious mice treated with a HFD for 26 wk during an euglycemic-hyperinsulinemic clamp (Fig. 2 *I*–*J*). During hyperinsulinemic conditions, Mfn2 KO mice showed a trend to enhance hepatic glucose production and to reduce glucose infusion rate compared with wild-type mice (Fig. 2*I*). During the clamp, incorporation of glucose into muscle glycogen was reduced in Mfn2 KO mice, although differences did not reach statistical significance (Fig. 2*J*). The absence of significant differences in insulin sensitivity between control and KO mice may be explained by the use of five mice per group, which underpowered these experiments compared with other studies, and by the long exposure of mice to a HFD. Altogether, our results indicate that deficient expression of Mfn2 in adult mice causes metabolic alterations that are associated with a higher susceptibility to insulin resistance in response to aging or to a HFD.

Mfn2 Deficiency Impairs Insulin Signaling in Liver, Skeletal Muscle, and Muscle Cells. On the basis of the impact of Mfn2 loss of function on glucose disposal and plasma insulin levels, we next tested whether Mfn2 affects insulin signaling in liver and in skeletal muscle. Defective hepatic insulin signaling [lower activation of insulin receptor substrate 1 (IRS1) and IRS2 association to the p85 subunit of PI3K or Akt phosphorylation] was detected in L-KO mice (Fig. 3*A* and Fig. S4*A*). The expression of the β-subunit of insulin receptors IRS1, p85 subunit of PI3K, or Akt was normal (Fig. 3*A* and Fig. S4*B*), and IRS2 was markedly repressed (Fig. S4*B*).

Soleus muscles from Mfn2-deficient mice subjected to chow diet were incubated in the absence or presence of insulin and then insulin-stimulated. Akt phosphorylation was analyzed. Muscles from control mice underwent a marked phosphorylation of Akt in response to insulin, and this effect was reduced in muscles of Mfn2-deficient mice (Fig. S4*C*). Similarly, insulin-stimulated Akt phosphorylation was blocked in soleus muscles of Mfn2-deficient mice subjected to a HFD (Fig. S4*D*). Defective insulin signaling (lower IRS1 association to the p85 subunit of PI3K or Akt phosphorylation but normal insulin receptor activation) was detected in Mfn2-deficient mice treated with a HFD in response to in vivo insulin administration (Fig. 3*B* and Fig. S4*E*). Insulin-induced p38 phosphorylation was not altered in muscles from Mfn2-deficient mice (Fig. S5*D*). To determine whether Mfn2 deficiency triggers an autonomous cellular response, Mfn2 was silenced in L6E9 muscle cells (Fig. S6*A*). Mfn2 knockdown muscle cells showed an impaired capacity to respond to insulin. Insulin-stimulated glucose transport was markedly blocked in these cells (Fig. S6*B*). Furthermore, Mfn2 knockdown cells showed impaired insulin signaling characterized by lower activation of Akt and IRS1 or a lower association of the p85 subunit of PI3K to IRS1, with no changes in insulin receptor phosphorylation (Fig. S6*C*). Overall,

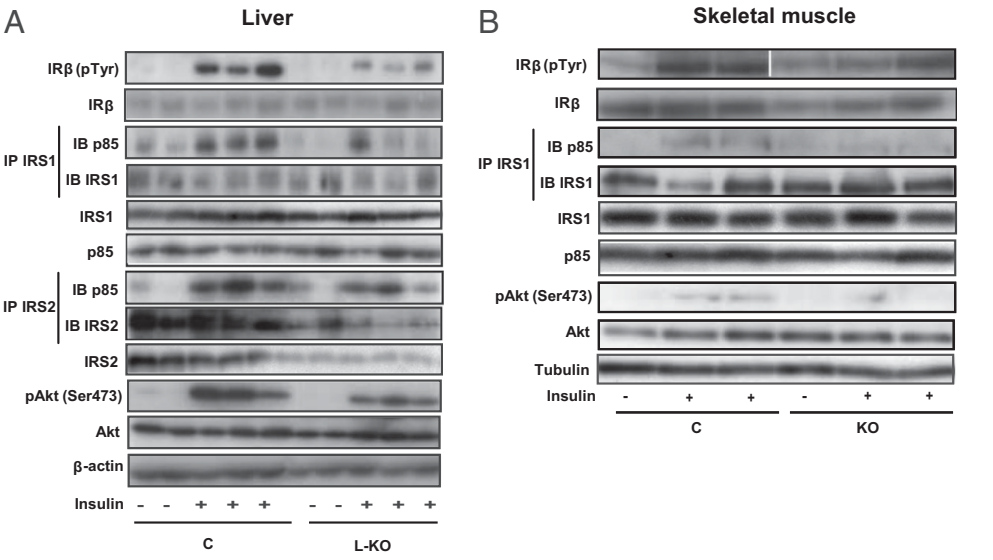

Fig. 3. Mfn2 loss-of-function impairs insulin signaling in liver and skeletal muscle in vivo. (*A*) Insulin receptor (IR) tyrosine phosphorylation, p85 subunit of PI3K bound to IRS1 or IRS2, and Akt phosphorylation were measured using specific antibodies in liver extracts from C or L-KO mice on a normal diet 5 min after portal vein insulin injection. (*B*) Insulin receptor (IR) tyrosine phosphorylation, p85 subunit of PI3K bound to IRS1, and Akt phosphorylation were measured in gastrocnemius extracts from C or KO mice on high-fat diet.

the pattern of alterations in insulin signaling was similar in Mfn2-silenced muscle cells and in muscle obtained from Mfn2-deficient mice.

Mfn2 Deficiency Causes Mitochondrial Dysfunction and Enhanced Hydrogen Peroxide Concentrations. We next analyzed whether Mfn2 deficiency caused mitochondrial dysfunction. Mfn2-ablated liver mitochondria exhibited a reduced state 4 and state 3 respiration (Fig. S7*A*) as well as reduced respiratory activities of complexes I + III or II + III (Fig. S7*B*). These changes occurred in the absence of alterations in the expression of subunits of respiratory complexes, mitochondrial DNA copy number, or ATP concentrations (Fig. S7 *C–E*). Under those conditions, the content of hydrogen peroxide was enhanced in liver upon Mfn2 depletion (Fig. S7*F*). This result occurred in the presence of reduced superoxide dismutase (SOD) and catalase activities as well as no changes in glutathione peroxidase (GPx) or glutathione reductase (GR) activities in L-KO mice (Fig. S7*G*) or in the reduced glutathione to oxidized glutathione (GSH/GSSG) ratio (Fig. S7*H*).

We have analyzed mitochondrial function in two models of muscle Mfn2 deficiency, i.e., Mfn2 KO mice and in mice electroporated with microRNA (miRNA). Skeletal muscles composed of mixed fast-twitch muscle fibers obtained from Mfn2 KO mice showed a reduced respiratory control ratio, which occurred in the absence of significant changes in state 3 and state 4 oxygen consumption (Fig. S8 *A* and *B*). Electroporation of miRNA caused a marked reduction of Mfn2 in mixed fast-twitch muscle fibers (Fig. S8*C*). Under these conditions, expression of protein subunits encoding for succinate dehydrogenase complex subunit A (SdhA; complex II) and cytochrome *c* oxidase subunit IV (Cox IV; complex IV) were repressed (Fig. S8*D*), and activity of respiratory complex IV was reduced in Mfn2-deficient muscles (Fig. S8*E*). Mfn2 ablation did not alter mitochondrial DNA copy number (Fig. S8*F*), the expression of porin, or ATP concentrations (Fig. S8*G*). Mfn2-ablated soleus muscles (enriched in slow-twitch oxidative fibers) showed reduced glucose oxidation (Fig. S8*H*), increased expression of protein subunits encoding for NADH dehydrogenase (ubiquinone) 1α subcomplex 9 (Ndufa9; complex I) and SdhA (complex II), as well as reduced expression of ubiquinol-cytochrome *c* reductase core protein 2 (Uqcrc2; complex III) and Cox IV (complex IV) (Fig. S8*I*).

Additional evidence indicating that Mfn2 deficiency causes mitochondrial dysfunction came from studies in muscle cells in culture. Mfn2-silenced muscle cells showed enhanced routine respiration, reduced respiratory control ratio, and enhanced respiratory leak in the absence of changes in ATP levels (Fig. S6 *E–H*). The content of hydrogen peroxide was also enhanced in skeletal muscle upon Mfn2 depletion (Fig. S8*J*) or in Mfn2-silenced muscle cells (Fig. S6*I*). These results occurred in the presence of enhanced GPx activity and no changes in SOD, catalase, or GR activities in Mfn2 KO mice (Fig. S8*K*) or in the GSH/GSSG ratio (Fig. S8*L*).

Mfn2 Deficiency Causes ER Stress and Activates JNK in Liver and Muscle. It has been reported that Mfn2 plays a key role in the tethering of ER to mitochondria (8). On the basis of this information, we analyzed the possible development of ER stress caused by Mfn2 deficiency. Livers from L-KO mice showed a marked increase in phosphorylated eukaryotic translation initiation factor 2α (eIF2α), DNA-damage inducible transcript 3 or Ddit3 (CHOP), and phosphorylated IRE1 (markers of ER stress) compared with controls (Fig. 4*A* and Fig. S9*A*). An increased abundance of ER stress markers such as phosphorylated eIF2α, CHOP, activating transcription factor 6 (ATF6), and GRP78 or glucose-regulated protein (BiP) was also detected in Mfn2-deficient skeletal muscle (Fig. 4*B* and S9*B*). Thus, our data indicate ER stress in liver and muscle under conditions of Mfn2 deficiency.

ER stress or reactive oxygen species (ROS) activate JNK, which, in turn, phosphorylates IRS proteins and inhibits insulin signaling (27–29). In light of this process and the enhanced hydrogen peroxide concentrations, we next analyzed the effects of Mfn2 depletion on JNK activation as well as on the phosphorylation of Ser^{307} in IRS1. Liver extracts obtained from L-KO mice showed higher activation of JNK and greater phosphorylation of Ser^{307} in IRS1 (Fig. 4 *C* and *D* and Fig. S9 *C* and *D*). Similarly, JNK phosphorylation was enhanced in Mfn2-deficient skeletal muscle or muscle cells, and an enhanced phosphorylation of Ser^{307} in IRS1 was also detected (Fig. 4 *E–G* and Fig. S9 *E–G*).

To determine whether JNK plays a role in the development of reduced insulin signaling under conditions of Mfn2 deficiency, control and Mfn2-silenced muscle cells were incubated with the selective JNK inhibitor SP600125 (30). This compound blocked JNK activation induced by Mfn2 silencing and normalized insulin-stimulated Akt phosphorylation (Fig. S9*F*) as well as Ser^{307} IRS1 phosphorylation (Fig. S9*G*). Altogether, our studies indicate that Mfn2 deficiency causes ER stress, mitochondrial dysfunction, hydrogen peroxide increase, and JNK activation, leading to altered insulin signaling in cells via phosphorylation of IRS1 at Ser^{307}.

Tauroursodeoxycholic Acid (TUDCA) or *N*-Acetylcysteine (NAC) Normalizes Insulin Signaling and Glucose Tolerance in Liver-Specific Mfn2 KO Mice. To demonstrate the role of ER stress in the maintenance of reduced insulin signaling and altered glucose

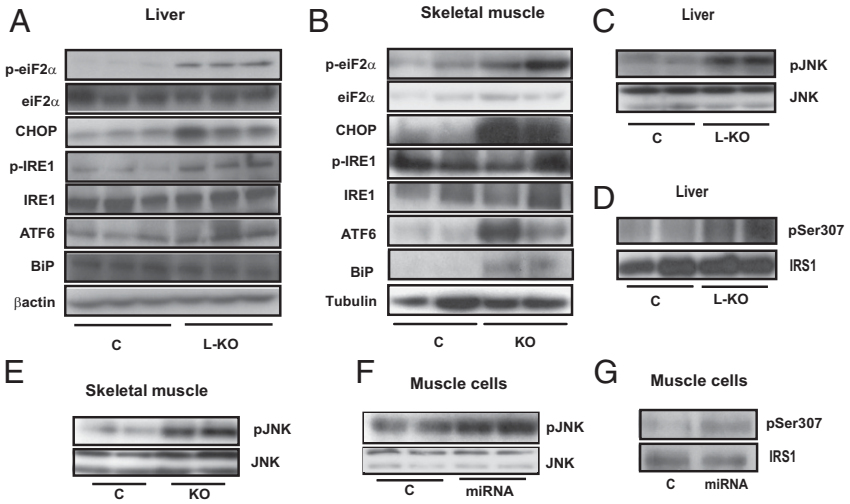

Fig. 4. Mfn2 ablation causes ER stress and JNK activation. (*A–B*) ER stress markers were evaluated in liver from C and L-KO mice (*A*) and in skeletal muscle from C and KO mice (*B*). (*C–G*) Western blot analysis of pJNK was performed in liver of C and L-KO mice (*C*), skeletal muscle from C and KO mice (*E*), and L6E9 myotubes (*F*). Ser 307 phosphorylation of IRS1 was analyzed in livers from C and L-KO mice (*D*) and L6E9 myotubes (*G*).

disposal in L-KO mice, we performed rescue studies with the chemical chaperone TUDCA. Wild-type or L-KO mice were treated or not treated with TUDCA for 3 wk as reported (31). As expected, TUDCA treatment normalized CHOP and phosphorylated IRE1 levels (Fig. S10*A*). TUDCA normalized JNK phosphorylation in L-KO mice and reduced hydrogen peroxide levels even below basal values in L-KO mice but not in controls (Fig. S10 *B–C*). Under these conditions, TUDCA also normalized Ser^{307} IRS1 phosphorylation and insulin-stimulated insulin receptor or Akt phosphorylation in L-KO mice (Fig. S10 *D–F* and Fig. S11). In keeping with this profile, TUDCA treatment also normalized glycemia and glucose tolerance of L-KO mice (Fig. S10 *G* and *H*). Altogether, our studies indicate that Mfn2 deficiency causes ER stress, and this process participates in the alterations of glucose disposal and deficient insulin-signaling in liver-specific Mfn2 KO mice.

Next we studied whether the metabolic effects linked to hepatic Mfn2 ablation were sensitive to antioxidants. Control and L-KO mice were treated for 3 wk with NAC in the drinking water (1% wt/vol). NAC treatment reduced hydrogen peroxide concentrations in control and L-KO mice so that differences between groups were no longer detectable (Fig. S12*A*). NAC treatment normalized CHOP levels and reduced phosphorylated IRE1 in L-KO mice below control values (Figs. S12*B* and S13). NAC also prevented the enhanced JNK phosphorylation in L-KO mice (Figs. S12*C* and S13). Under these conditions, NAC normalized Ser^{307} IRS1 phosphorylation or Akt phosphorylation in L-KO mice, whereas it only partially rescued insulin receptor phosphorylation (Figs. S12 *D–F* and S13). Furthermore, NAC treatment also normalized glycemia and glucose tolerance of L-KO mice (Fig. S12 *G* and *H*).

Discussion

A major conclusion of this study is that Mfn2 regulates insulin signaling and insulin sensitivity in muscle and liver tissues. Here, we demonstrate that Mfn2 deficiency in mice induces susceptibility to develop insulin resistance in response to both age and HFD treatment. These data fit with the observations that muscle Mfn2 is repressed in human obesity or in type 2 diabetes (13, 14) and allow us to propose that Mfn2 is a regulator of in vivo insulin sensitivity and a potential target in diabetes drug development.

L-KO mice showed glucose intolerance, which is, at least in part, attributable to an increased hepatic gluconeogenesis. In this regard, we detected an increased expression of gluconeogenic genes, such as pyruvate carboxylase, PEPCK, and glucose 6-phosphatase, and regulators of gluconeogenesis, such as PGC-1α (32), in livers from L-KO mice. In addition, an increased capacity to dephosphorylate and, consequently, reactivate CRTC2 in response to short-term fasting as well as a reduced capacity of insulin to phosphorylate and, therefore, inhibit FoxO1 were observed in livers from L-KO mice. Given the capacity of PGC-1α and CRTC2 to coactivate CREB (25, 33, 34), as well as the observations that ER stress triggers the dephosphorylation of CRTC2 in cultured cells (35), we favor the idea that Mfn2 loss of function triggers ER stress, which causes dephosphorylation of CRTC2 and further activation of CREB.

Mfn2 deficiency in skeletal muscle was associated with a pattern of insulin resistance in 12-mo-old mice and glucose intolerance after HFD. Under these conditions, euglycemic-hyperinsulinemic clamp studies suggested a higher rate of hepatic glucose production and reduced glycogen synthesis in muscle from Mfn2 KO mice. Whether the hepatic changes are because of the fact that Mfn2 is downregulated in livers from Mfn2 KO mice deserves further analysis.

Mfn2 deficiency reduces insulin signaling in muscle and liver tissues and induces susceptibility to develop insulin resistance. In this connection, we provide evidence that Mfn2 deficiency causes enhanced hydrogen peroxide concentrations, altered ROS handling, and mitochondrial dysfunction in both liver and muscle. In parallel with a greater ROS production, Mfn2 deficiency caused enhanced JNK phosphorylation as well as higher phosphorylation of IRS1 at Ser^{307}, which is consistent with prior findings indicating that ROS activates JNK through apoptosis signal-regulating kinase 1 (ASK1) and that JNK phosphorylates and inactivates IRS proteins at Ser^{307} (27–29). Additional demonstration of the concept that Mfn2 deficiency leads to insulin resistance via ROS production and JNK activation came from the use of the antioxidant compound NAC or the JNK inhibitor SP600125. Incubation of Mfn2-silenced muscle cells with SP600125 normalized Ser^{307} phosphorylation of IRS1 and insulin-stimulated Akt phosphorylation. Furthermore, chronic treatment with NAC normalized insulin signaling and glucose tolerance in L-KO mice. Altogether, our data support the view that Mfn2 deficiency causes mitochondrial dysfunction, which leads to enhanced ROS production, enhanced JNK activity, and inactivation of IRS1, a key protein in insulin signaling.

Mfn2 ablation caused mitochondrial dysfunction as well as alterations in mitochondrial morphology both in liver and in skeletal muscle. Hepatocytes from L-KO mice showed mitochondria that were organized in clumps rather than showing a normal elongated morphology. Transmission electron microscopic observation of hepatic ultrathin sections confirmed the increased presence of spherical mitochondria in L-KO mice. The existence of larger mitochondria was also detected by electron microscopy in skeletal muscles from Mfn2 KO mice. Alterations in mitochondrial morphology associated with Mfn2 ablation have also been reported in cardiomyocytes (36), Purkinje cells (37), and mouse embryo fibroblasts (38). Mitochondria are usually larger in diameter and appear round upon ablation of Mfn2 compared with the elongated, tubular mitochondria detected in control conditions, and this

alteration occurs in different cell types. These observations suggest that, in addition to supporting mitochondrial fusion, Mfn2 is involved in other roles that control mitochondrial size.

Another major finding of our study is that Mfn2 loss of function triggers ER stress in liver and in skeletal muscle. This finding seems to be relevant in many of the metabolic alterations detected in the liver-specific Mfn2 KO mouse because chronic treatment with the chemical chaperone TUDCA, which reduces hepatic ER stress, normalized the alterations in insulin signaling and glucose disposal in that animal model. Our data are in agreement with the report by de Brito and Scorrano stating that Mfn2 tethers ER to mitochondria and regulates calcium homeostasis in cells (8). In this regard, we propose that Mfn2 deficiency in liver and muscle causes a defective calcium homeostasis, which may be instrumental in the development of ER stress. In keeping with this view, hepatocytes from L-KO mice show increased cytosolic calcium levels in response to inhibition of sarcoplasmic reticulum/ER Ca^{2+}-ATPase (SERCA) activity induced by thapsigargin. This observation suggests greater calcium storage in the ER of cells lacking Mfn2, a notion that is consistent with data obtained in mouse embryo fibroblasts (8).

In summary, we propose a model by which Mfn2 regulates insulin signaling in skeletal muscle and liver through mechanisms that depend on ROS production and ER stress. In in vivo studies, we found that both ROS and ER stress played major roles contributing to deficient insulin signaling, and either NAC or TUDCA normalized JNK, insulin signaling, or glucose tolerance in liver-specific Mfn2 KO mice. Our data additionally indicate the existence of a bidirectional positive cross-talk between ER stress and ROS that is activated only under conditions of Mfn2 deficiency and results in activation of JNK, causing insulin resistance. This finding is in keeping with previous observations indicating that ER and mitochondria undergo a complex relationship in response to ER stress (39).

Materials and Methods

Animal Care, Generation of Animal Models, and Diet Treatments. All animal work was performed in compliance with guidelines established by the University of Barcelona Committee on Animal Care. $Mfn2^{loxP/loxP}$ mice were provided by David Chan (Division of Biology and Howard Hughes Medical Institute, California Institute of Technology, Pasadena, CA) ($Mfn2^{tm3Dcc}$/Mmcd) (37) through Mutant Mouse Regional Resource Center. Homozygous $Mfn2^{loxP/loxP}$ mice were crossed with different mouse strains expressing Cre recombinase. See *SI Materials and Methods* for further details.

Respiration Studies in Permeabilized Muscle, Isolated Liver Mitochondria, or Cultured Muscle Cells. The respiration of permeabilized muscle fibers and liver mitochondria was measured at 37 °C by high-resolution respirometry with the Oxygraph-2k (Oroboros Instruments). Respirometry of cultured muscle cells was performed with the Seahorse Bioscience XF 24 platform. See *SI Materials and Methods* for further details.

ACKNOWLEDGMENTS. This study was supported by Ministerio de Educación y Cultura Grant SAF2008-03803; Generalitat de Catalunya, Instituto de Salud Carlos III, Centro de Investigación Biomédica en Red de Diabetes y Enfermedades Metabólicas Asociadas (CIBERDEM) Grant 2009SGR915; European Commission Seventh Framework Programme (FP7), Integration of the System Models of Mitochondrial Function and Insulin Signalling and its Application in the Study of Complex Diseases (MITIN) Grant HEALTH-F4-2008-223450; and Innovation and Environment Regions of Europe Sharing Solutions (INTERREG) IV-B/Le Programme de Coopération Territoriale de l'Espace Sud-Ouest Européen (SUDOE)/Fonds Européen de Développement Régional (FEDER), Transnational Cooperation for Technological Innovation in the Development of Molecules for the Treatment of Diabetes and Obesity (DIOMED) Grant SOE1/P1/E178. J.S. and M.I.H.-A. were recipients of predoctoral fellowships from the Fundación Ramon Areces, Spain, and from the El Consejo Nacional de Ciencia y Tecnología (CONACYT), Mexico, respectively. D. Sala, M.L., and J.C.P. were recipients of predoctoral fellowships from the Ministerio de Educación y Cultura, Spain. A.Z. is the recipient of a Science Intensification Award from the University of Barcelona.

1. Liesa M, Palacín M, Zorzano A (2009) Mitochondrial dynamics in mammalian health and disease. *Physiol Rev* 89:799–845.
2. Twig G, et al. (2008) Fission and selective fusion govern mitochondrial segregation and elimination by autophagy. *EMBO J* 27:433–446.
3. Yasukawa K, et al. (2009) Mitofusin 2 inhibits mitochondrial antiviral signaling. *Sci Signal* 2:ra47.
4. Pich S, et al. (2005) The Charcot-Marie-Tooth type 2A gene product, Mfn2, up-regulates fuel oxidation through expression of OXPHOS system. *Hum Mol Genet* 14:1405–1415.
5. Hailey DW, et al. (2010) Mitochondria supply membranes for autophagosome biogenesis during starvation. *Cell* 141:656–667.
6. Chen KH, et al. (2004) Dysregulation of HSG triggers vascular proliferative disorders. *Nat Cell Biol* 6:872–883.
7. Bach D, et al. (2003) Mitofusin-2 determines mitochondrial network architecture and mitochondrial metabolism. A novel regulatory mechanism altered in obesity. *J Biol Chem* 278:17190–17197.
8. de Brito OM, Scorrano L (2008) Mitofusin 2 tethers endoplasmic reticulum to mitochondria. *Nature* 456:605–610.
9. Chen H, et al. (2010) Mitochondrial fusion is required for mtDNA stability in skeletal muscle and tolerance of mtDNA mutations. *Cell* 141(2):280–289.
10. Chung KW, et al. (2006) Early onset severe and late-onset mild Charcot-Marie-Tooth disease with mitofusin 2 (MFN2) mutations. *Brain* 129:2103–2118.
11. Verhoeven K, et al. (2006) MFN2 mutation distribution and genotype/phenotype correlation in Charcot-Marie-Tooth type 2. *Brain* 129:2093–2102.
12. Züchner S, et al. (2004) Mutations in the mitochondrial GTPase mitofusin 2 cause Charcot-Marie-Tooth neuropathy type 2A. *Nat Genet* 36:449–451.
13. Bach D, et al. (2005) Expression of Mfn2, the Charcot-Marie-Tooth neuropathy type 2A gene, in human skeletal muscle: Effects of type 2 diabetes, obesity, weight loss, and the regulatory role of tumor necrosis factor α and interleukin-6. *Diabetes* 54:2685–2693.
14. Hernández-Alvarez MI, et al. (2010) Subjects with early-onset type 2 diabetes show defective activation of the skeletal muscle PGC-1α/Mitofusin-2 regulatory pathway in response to physical activity. *Diabetes Care* 33:645–651.
15. Lillioja S, et al. (1993) Insulin resistance and insulin secretory dysfunction as precursors of non-insulin-dependent diabetes mellitus. Prospective studies of Pima Indians. *N Engl J Med* 329:1988–1992.
16. Kelley DE, He J, Menshikova EV, Ritov VB (2002) Dysfunction of mitochondria in human skeletal muscle in type 2 diabetes. *Diabetes* 51:2944–2950.
17. Mogensen M, et al. (2007) Mitochondrial respiration is decreased in skeletal muscle of patients with type 2 diabetes. *Diabetes* 56:1592–1599.
18. Petersen KF, et al. (2003) Mitochondrial dysfunction in the elderly: Possible role in insulin resistance. *Science* 300:1140–1142.
19. Petersen KF, Dufour S, Befroy D, Garcia R, Shulman GI (2004) Impaired mitochondrial activity in the insulin-resistant offspring of patients with type 2 diabetes. *N Engl J Med* 350:664–671.
20. Garcia-Roves P, et al. (2007) Raising plasma fatty acid concentration induces increased biogenesis of mitochondria in skeletal muscle. *Proc Natl Acad Sci USA* 104: 10709–10713.
21. Turner N, et al. (2007) Excess lipid availability increases mitochondrial fatty acid oxidative capacity in muscle: Evidence against a role for reduced fatty acid oxidation in lipid-induced insulin resistance in rodents. *Diabetes* 56:2085–2092.
22. Pospisilik JA, et al. (2007) Targeted deletion of AIF decreases mitochondrial oxidative phosphorylation and protects from obesity and diabetes. *Cell* 131:476–491.
23. Anderson EJ, et al. (2009) Mitochondrial H_2O_2 emission and cellular redox state link excess fat intake to insulin resistance in both rodents and humans. *J Clin Invest* 119:573–581.
24. Bonnard C, et al. (2008) Mitochondrial dysfunction results from oxidative stress in the skeletal muscle of diet-induced insulin-resistant mice. *J Clin Invest* 118:789–800.
25. Herzig S, et al. (2001) CREB regulates hepatic gluconeogenesis through the coactivator PGC-1. *Nature* 413(3):179–183.
26. Heidt AB, Black BL (2005) Transgenic mice that express Cre recombinase under control of a skeletal muscle-specific promoter from *mef2c*. *Genesis* 42(1):28–32.
27. Aguirre V, et al. (2002) Phosphorylation of Ser^{307} in insulin receptor substrate-1 blocks interactions with the insulin receptor and inhibits insulin action. *J Biol Chem* 277:1531–1537.
28. Ichijo H, et al. (1997) Induction of apoptosis by ASK1, a mammalian MAPKKK that activates SAPK/JNK and p38 signaling pathways. *Science* 275(2):90–94.
29. Lee YH, Giraud J, Davis RJ, White MF (2003) c-Jun N-terminal kinase (JNK) mediates feedback inhibition of the insulin signaling cascade. *J Biol Chem* 278:2896–2902.
30. Bennett BL, et al. (2001) SP600125, an anthrapyrazolone inhibitor of Jun N-terminal kinase. *Proc Natl Acad Sci USA* 98:13681–13686.
31. Ozcan U, et al. (2004) Endoplasmic reticulum stress links obesity, insulin action, and type 2 diabetes. *Science* 306:457–461.
32. Yoon JC, et al. (2001) Control of hepatic gluconeogenesis through the transcriptional coactivator PGC-1. *Nature* 413(5296):131–138.
33. Conkright MD, et al. (2003) TORCs: Transducers of regulated CREB activity. *Mol Cell* 12:413–423.
34. Iourgenko V, et al. (2003) Identification of a family of cAMP response element-binding protein coactivators by genome-scale functional analysis in mammalian cells. *Proc Natl Acad Sci USA* 100:12147–12152.
35. Wang Y, Vera L, Fischer WH, Montminy M (2009) The CREB coactivator CRTC2 links hepatic ER stress and fasting gluconeogenesis. *Nature* 460:534–537.
36. Papanicolaou KN, et al. (2011) Mitofusin-2 maintains mitochondrial structure and contributes to stress-induced permeability transition in cardiac myocytes. *Mol Cell Biol* 31:1309–1328.
37. Chen H, McCaffery JM, Chan DC (2007) Mitochondrial fusion protects against neurodegeneration in the cerebellum. *Cell* 130:548–562.
38. Chen H, et al. (2003) Mitofusins Mfn1 and Mfn2 coordinately regulate mitochondrial fusion and are essential for embryonic development. *J Cell Biol* 160(21):189–200.
39. De Raedt T, et al. (2011) Exploiting cancer cell vulnerabilities to develop a combination therapy for Ras-driven tumors. *Cancer Cell* 20:400–413.